Metabolism of Furans in Vitro: Ipomeanine and 4-Ipomeanol

Ling-Jen Chen,*,† Eugene F. DeRose,‡ and Leo T. Burka†

Laboratory of Pharmacology and Chemistry, and Laboratory of Structural Biology, National Institute of Environmental Health Sciences, Research Triangle Park, North Carolina 27709

Received June 13, 2006

Ipomeanine (IPN), 4-ipomeanol (4-IPO), 1-ipomeanol (1-IPO), and 1,4-ipomeadiol (DIOL) are toxic 3-substituted furans found in mold-damaged sweet potatoes. IPN and 4-IPO are the most toxic, but all produce pulmonary toxicity in cattle and rodents, and 4-IPO induces hepatotoxicity in humans. These furans require metabolic activation to elicit toxicity, but the limited information obtained from previous metabolism studies prompted us to initiate the investigation reported here. Our initial studies of 4-IPO metabolism by rat liver microsomes demonstrated that the oxidation of 4-IPO to IPN and reduction to DIOL occurred and that more IPN was metabolized to a reactive species than 4-IPO or DIOL. Incubation of IPN and Gly produced a 2′-pyrrolin-5′-one adduct establishing that IPN was metabolized to an enedial. *N*-Acetylcysteine reacted with the 5′-aldehyde of the enedial to give two 2′,5′-dihydro-2′-hydroxyfurans stabilized by H bonding between the 2′-OH and 3′-keto group. Reaction of the enedial metabolite of IPN with one GSH gave several adducts including a pyrrole derived from the 1,2-addition of GSH to the 5′-aldehyde as well as two tricyclic 2′-pyrrolines derived from the 1,4-addition of GSH at the 4′-position. The identities of the pyrrole and 2′-pyrroline GSH adducts were confirmed by observation of structurally similar adducts from Cys conjugation with the enedial metabolite of IPN. Several minor adducts from the conjugation of the enedial metabolite of IPN with two GSH were also detected. Mono-GSH and bis-GSH adducts were derived from both the 1,2-and 1,4-addition of GSH to the enedial metabolite of 4-IPO in rat liver microsomal incubations of 4-IPO and GSH. Sequential oxidation of 4-IPO to IPN and then to the enedial metabolite followed by GSH conjugation also occurred in the 4-IPO incubations. The complex structures of the reaction products of the enedial with biological nucleophiles may explain why the many attempts to identify 4-IPO adducts to protein have not been successful.

Introduction

Ipomeanine (IPN[11], 1-(3′-furyl)-1,4-pentanedione), 4-ipomeanol (4-IPO, 1-(3′-furyl)-4-hydroxy-1-pentanone), 1-ipomeanol (1-IPO, 1-(3′-furyl)-1-hydroxy-4-pentanone), and 1,4-ipomeadiol (DIOL, 1-(3′-furyl)-1,4-pentanediol) (Figure 1) are four 3-substituted furans responsible for the pulmonary toxicity that sometimes occurred when cattle were fed mold-damaged sweet potatoes (*1*, *2*). These furans are degradation products of furanosesquiterpenoid metabolites that sweet potatoes produce in response to fungal infection or other stress (*3*). All four 3-substituted furans cause pulmonary toxicity in mice similar to that seen in cattle. The oral LD_{50} values in mice for IPN, 4-IPO, 1-IPO, and DIOL are 26 ± 1, 38 ± 3, 79 ± 9, 104 ± 12 mg/kg, respectively (*2*). Of the four furans, 4-IPO has received the most attention, including a clinical trial for the treatment of lung cancer. 4-IPO-treated patients developed severe hepatotoxicity with little toxicity to the lungs or the lung cancer (*4*).

4-IPO is bioactivated by lung or liver microsomes and NADPH to a metabolite that reacts with proteins and forms stable adducts with GSH (*5*, *6*). Induction of cytochromes P450 by the pretreatment of rodents with 3-methylcholanthrene shifts toxicity to the liver, presumably by increasing metabolism in that organ (*7*). Only recently has an enedial metabolite from the bioactivation of 4-IPO been characterized. Alvarez-Diez and Zheng (*8*) reported an in vivo metabolism study of 4-IPO in bile-duct-cannulated rats. They detected four biliary metabolites that were characterized by MS monitoring at *m*/*z* 492 ($M + H^+$), equivalent to adduction between the enedial metabolite (184) and one GSH (307). The proposed aldehyde-containing structures for these adducts, however, seemed improbable and prompted us to begin the studies reported here. Recently, Baer et al. (*9*) reported that in vitro metabolism of 4-IPO by rabbit CYP4B1, NADPH, and GSH gave two bis-GSH pyrrole adducts from conjugation of the enedial metabolite with two GSH followed by the loss of two H_2O molecules. Multiple human liver P450s that are capable of the 4-IPO bioactivation were also identified (*9*).

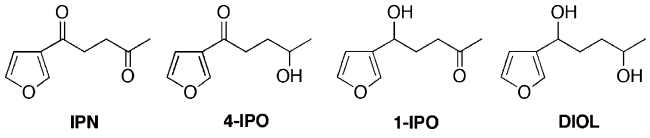

Figure 1. Structures of ipomeanine (IPN), 4-ipomeanol (4-IPO), 1-ipomeanol (1-IPO), and 1,4-ipomeadiol (DIOL).

The metabolism of furans to a 1,4-dicarbonyl moiety is well established for furan and furans substituted with only alkyl groups. The microsomal metabolism of 2- and 3-methylfurans to acetylacrolein and 2-methylbutene-1,4-dial were the first examples (*10*). McClanahan et al. (*11*), subsequently, demon-

* Corresponding author. Tel: 919-541-2959. Fax: 919-541-1885. E-mail: ferguso2@niehs.nih.gov.

† Laboratory of Pharmacology and Chemistry.

‡ Laboratory of Structural Biology.

[1] Abbreviations: IPN, ipomeanine; 4-IPO, 4-ipomeanol; 1-IPO, 1-ipomeanol; DIOL, 1,4-ipomeadiol; AcCys, *N*-acetylcysteine; ESI-MS, electrospray ionization-mass spectrometry; ESI-MS/MS, electrospray ionization-tandem mass spectrometry; DQF COSY, double-quantum-filtered correlation spectroscopy; TROESY, transverse rotating frame Overhauser effect spectroscopy; HSQC, heteronuclear single-quantum correlation; MW, molecular weight.

10.1021/tx060128f CCC: $33.50
Published on Web 09/02/2006

strated that the metabolism of menthofuran resulted in the oxidation of the furan to a ketoenal. The oxidation of furan to *cis*-2-butene-1,4-dial was demonstrated by Chen et al. (*12*). These studies relied on trapping the intermediates with semicarbazide. The products from the reaction of *cis*-2-butene-1,4-dial with amino acids and GSH have been extensively studied (*13*, *14*). Studies in vivo where metabolites derived from the oxidation of furan were identified are limited to the Alvarez-Diez and Zheng study with 4-IPO (*8*) and the identification of menthofuran metabolites, 2-(glutathion-*S*-yl)menthofuran (*15*) and hexahydro-3,6-dimethyl-1-(2-sulfoethyl)-2*H*-indol-2-one (*16*). The latter metabolite is the taurine adduct of the ketoenal.

The characterization of GSH adducts in recent studies of 4-IPO prompted a reinvestigation of 4-IPO metabolism. This effort has demonstrated that the major metabolic processes in rat liver microsomal incubations include oxidation and reduction of 4-IPO to IPN and DIOL, respectively. The reduction of IPN to 4-IPO in microsomal incubations was also observed. The IPN to 4-IPO interconversion is likely to occur in vivo, and information gained from IPN studies is applicable to 4-IPO. There was no published metabolism study for IPN, and therefore, the present study includes metabolism studies of both IPN and 4-IPO.

Experimental Procedures

Materials. IPN, 4-IPO, and DIOL were prepared as described previously (*2*). Trifluoroacetic acid, glucose 6-phosphate, glucose-6-phosphate dehydrogenase, $NADP^+$, Gly, Cys, *N*-acetylcysteine (AcCys), and GSH were obtained from Sigma-Aldrich Co. (St. Louis, MO). Male F344 rat liver microsomes (20 mg protein/mL) were purchased from In Vitro Technologies (Baltimore, MD).

Instrumentation. HPLC analyses were carried out on a Beckman System Gold module 126 solvent pump, a module 168 photodiode array detector. A gradient from 100% 0.1% trifluoroacetic acid in H_2O to 25% CH_3CN over 25 min, then held for 5 min at a flow rate of 1.5 mL/min on a Metachem (Torrance, CA) Inertsil C18 5 μm column (4.6 × 250 mm) was used for analysis and isolation of the products in the incubations.

Electrospray ionization mass spectra (ESI-MS) were obtained on a Thermo Finnigan LCQ DUO ion trap mass spectrometer (Riviera Beach, FL). Tandem mass spectra (ESI-MS/MS) were produced by collision-induced dissociation of the selected parent ions with the helium gas present in the mass analyzer. The heated capillary was maintained at 200 °C and the source voltage at 4.5 kV.

One-dimensional ^1H NMR spectra were acquired on Varian Gemini 300 MHz or INOVA 500 MHz NMR spectrometers (Palo Alto, CA). The chemical shifts are reported in ppm relative to solvents (D_2O at 4.80 ppm and acetone-d_6 at 2.05 ppm). Two-dimensional ^1H-^1H DQF COSY (*17*) and TROESY (*18*) experiments were acquired at 500 MHz. In these experiments, the ^1H sweep width was set at 12.8 ppm in each dimension, and 256 × 1024 complex points were acquired in the t_1 and t_2 dimensions, respectively. The TROESY experiment was obtained with a mixing time of 150 ms and a B1 field of 250 Hz, using 180°(x) 180°(−x) pulses. A ^1H-^{13}C HSQC (*19*, *20*) experiment was acquired at 500 MHz. In this experiment, the ^1H sweep width was 12.8 ppm, and the ^{13}C sweep width was 140 ppm, and 128 × 1024 complex points were acquired in the t_1 and t_2 dimensions, respectively.

Oxidation of IPN by Dimethyldioxirane-d_6. Dimethyldioxirane-d_6 was prepared as described (*21*). The reaction of IPN (7.1 mg, 0.043 mmol) with dimethyldioxirane-d_6 in acetone-d_6 (0.05 M, 0.85 mL, 0.043 mmol) in a NMR tube was monitored by ^1H NMR spectroscopy (300 MHz) at 25 °C. The following signals, consistent with enedial **1**, were observed in the spectrum: δ 10.25 (d, J = 5.8 Hz, 1H, 5′-H), 10.21 (d, J = 1.7 Hz, 1H, 2′-H), and 6.95 (dd, J = 6.1, 1.7 Hz, 1H, 4′-H); the other signals overlapped with the signals of IPN. A hydrate of **1** was also detected in the ^1H NMR spectrum. The hydrate existed as two isomers in a 1.7:1 ratio: the major isomer, δ 5.56 (s, 1H, 2′-H), 5.48 (d, J = 7.5 Hz, 1H, 5′-H), 5.00 (d, J = 7.7 Hz, 1H, 4′-H) and the minor isomer, δ 5.60 (s, 1H, 2′-H), 5.41 (d, J = 8.1 Hz, 1H, 5′-H), 5.02 (d, J = 7.4 Hz, 1H, 4′-H); the other signals overlapped with the signals of IPN.

General Procedure for the Incubations of IPN with Rat Liver Microsomes and NADPH in the Presence of Gly, AcCys, Cys, or GSH. Incubations of IPN (1 mM) with male F344 rat liver microsomes (2 mg protein/mL) were conducted in a 0.1 M potassium phosphate buffer (pH 7.4) in the presence of 3 mM $MgCl_2$, 25 mM glucose-6-phosphate, glucose-6-phosphate dehydrogenase (2 units/mL), 4 mM $NADP^+$, and 5 mM Gly (or AcCys, Cys or GSH). IPN was added as a CH_3CN solution (100 mM, 10 μL). The final volume was 1 mL, and the incubation took place at 37 °C in capped vials for 3 h (1 h for the AcCys experiment). The reactions were terminated by the addition of 0.3 N $Ba(OH)_2$ (0.1 mL) and 0.3 N $ZnSO_4$ (0.1 mL). Control experiments omitting either $NADP^+$ or Gly (or other trapping chemicals) were included so as to recognize the products. Following centrifugation, the supernatant was filtered through a Millex-HV syringe driven filter (Millipore Corporation, Bedford, MA; 0.45 μm, 13 mm), and the filtrate was analyzed by HPLC.

The incubations were scaled up to 10 mL for the isolation of the products using HPLC and the solvents were evaporated by a Speed-Vac (ThermoSavant, Holbrook, NY) before analysis by MS and/or ^1H NMR spectroscopy. Samples were dissolved in CH_3OH-H_2O (1:1) and introduced to the mass spectrometer through direct infusion (2.5−25 μL/min) for negative ionization analysis (ESI(−)-MS or ESI(−)-MS/MS) or positive ionization analysis (ESI(+)-MS or ESI(+)-MS/MS). Acetic acid, equivalent to 2% by volume, was added to some of the samples in CH_3OH-H_2O (1:1) for positive ionization analysis. ^1H NMR analysis was performed on samples with sufficient abundance.

1. Gly. One major product (**2**) eluting at 14.5 min was observed by HPLC analysis. **2** had the following spectral properties: UV: λ_{max} 223 and 295 (major) nm; ESI(−)-MS/MS: m/z 238 ($M - H^+$), 220 ($M - H^+ - H_2O$), 194 ($M - H^+ - CO_2$); ESI(+)-MS/MS: m/z 240 ($M + H^+$), 222 ($M + H^+ - H_2O$), 142 ($M + 2\ H^+ - COCH_2CH_2COCH_3^+$), 99 ($COCH_2CH_2COCH_3^+$); ^1H NMR (D_2O, 300 MHz): δ 7.93 (s, 1H, 2′-H), 4.18 (s, 2H, Gly α-CH_2), 3.37 (s, 2H, 4′-CH_2), 3.01 (t, J = 7.0 Hz, 2H, 2-CH_2), 2.89 (t, J = 6.6 Hz, 2H, 3-CH_2), 2.25 (s, 3H, 5-CH_3).

2. AcCys. Two products (**3a** and **3b**) eluting at 16.3 and 16.4 min were observed by HPLC. **3a** and **3b** had an identical UV absorption maximum (λ_{max} 263 nm) and were collected from HPLC in one fraction for MS analysis: ESI(−)-MS/MS: m/z 344 ($M - H^+$), 326 ($M - H^+ - H_2O$), 300 ($M - H^+ - CO_2$), 215 ($M - CH_2CH(NHCOCH_3)COOH^+$), 162 (AcCys anion); ESI(+)-MS/MS: m/z 346 ($M + H^+$), 328 ($M + H^+ - H_2O$), 304 ($M + H^+ - COCH_2$).

3. Cys. Two minor products eluting at 15.7 min (**4a**) and 16.3 min (**4b**) and two major products eluting at 16.7 min (**4c**) and 27.6 min (**5**) were observed by HPLC. The UV spectra of **4a**−**c** were similar: **4a**: λ_{max} 314 nm, **4b**: λ_{max} 304 nm, and **4c**: λ_{max} 304 nm. **4a**−**c** were collected from HPLC separately for MS. The results were similar for these three products: ESI(−)-MS/MS: m/z 387 ($M - H^+$), 343 ($M - H^+ - CO_2$), 309 ($M - H^+ - CO_2 - H_2S$), 291 ($M - H^+ - CO_2 - H_2S - H_2O$), 266 ($M - H^+ - Cys$), 222 ($M - H^+ - Cys - CO_2$); ESI(+)-MS/MS: m/z 389 ($M + H^+$), 371 ($M + H^+ - H_2O$), 353 ($M + H^+ - 2\ H_2O$), 343 ($M + H^+ - HCOOH$), 300 ($M + H^+ - H_2O - CH_2CH_2COCH_3$), 291 ($M + 2\ H^+ - COCH_2CH_2COCH_3^+$), 282 ($M + H^+ - 2\ H_2O - CH_2CH_2COCH_3$), 250 ($M + H^+ - Cys - H_2O$). Only **4c** was abundant enough for a ^1H NMR (D_2O, 300 MHz) spectrum: δ 7.61 (s, 1H, 2′-H), 5.35 (s, 1H, 5′-H), 4.97 (dd, J = 7.7, 1.7 Hz, 1H, Cys α-CH), 4.02 (t, J = 5.5 Hz, 1H, Cys α-CH), 3.34 (dd, J = 11.3, 1.5 Hz, 1H, Cys β-CH_a), 3.24 (d, J = 5.8 Hz, 2H, Cys β-CH_2), 3.17 (t, J = 7.4 Hz, 2H, 2-CH_2), 2.94 (t, J = 6.3 Hz, 2H, 3-CH_2), 2.93 (dd, J = 11.7, 7.4 Hz, 1H, Cys β-CH_b), 2.25 (s, 3H, 5-CH_3). There was a trace amount of a rearranged product (**6**) present in the ^1H NMR spectrum of **4c**: δ 7.92 (d, J = 2.1 Hz, 1H, 2′-H), 7.14 (d, J = 2.2

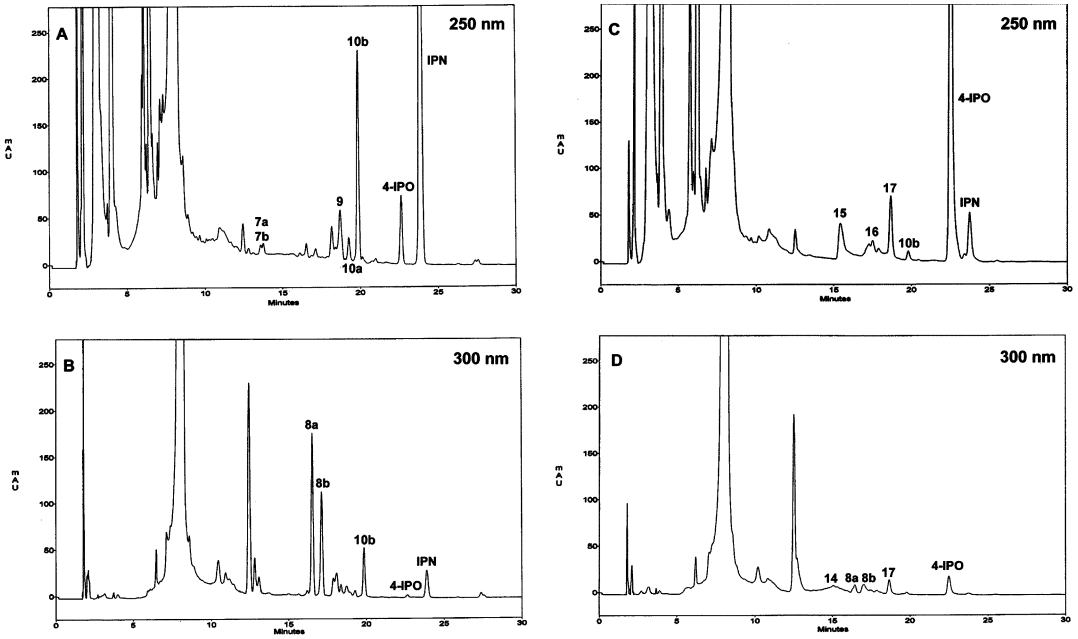

Figure 2. Representative UV chromatograms of rat liver microsomal incubation mixtures (100 μL each) of IPN at 250 nm (A) and 300 nm (B) or 4-IPO at 250 nm (C) and 300 nm (D).

Hz, 1H, 5′-H), 2.29 (s, 3H, 5-CH_3); the other signals overlapped with the signals of **4c**.

The spectral properties of **5** were as follows: UV: λ_{max} 231 (major) and 308 nm. ESI(−)-MS/MS: *m/z* 266 ($M - H^+$), 222 ($M - H^+ - CO_2$); ESI(+)-MS/MS: *m/z* 268 ($M + H^+$), 250 ($M + H^+ - H_2O$), 170 ($M + 2\,H^+ - COCH_2CH_2COCH_3^+$), 99 ($COCH_2$-$CH_2COCH_3^+$). ^{1}H NMR ($D_2O$, 300 MHz): δ 7.77 (s, 1H, 2′-H), 6.31 (s, 1H, 4′-H), 5.07 (dd, $J = 7.7$, 3.9 Hz, 1H, Cys α-CH), 4.12 (dd, $J = 11.5$, 7.7 Hz, 1H, Cys β-CH_a), 3.86 (dd, $J = 11.5$, 3.9 Hz, 1H, Cys β-CH_b), 3.13 (t, $J = 6.3$ Hz, 2H, 2-CH_2), 2.93 (t, $J = 6.3$ Hz, 2H, 3-CH_2), 2.27 (s, 3H, 5-CH_3).

4. GSH. Several peaks with a distinctive UV absorption at 260−320 nm (**7a**−**b**, **8a**−**b**, **9**, and **10a**−**b**) were observed by HPLC as shown in Figure 2A and B. These peaks were collected from HPLC along with the fraction at 17.9−18.4 min for ESI-MS and/or ^{1}H NMR spectra. The spectral properties were as follows.

7a and 7b. HPLC retention time 13.6 and 13.7 min; UV: λ_{max} 262 nm. **7a** and **7b** were collected from HPLC in one fraction for MS: ESI(−)-MS/MS: *m/z* 488 ($M - H^+$), 470 ($M - H^+ - H_2O$); ESI(+)-MS/MS: *m/z* 490 ($M + H^+$), 472 ($M + H^+ - H_2O$), 454 ($M + H^+ - 2\,H_2O$), 415 ($M + H^+ -$ Gly), 361 ($M + H^+ - 129$ (Glu)), 343 ($M + H^+ - 129$ (Glu) $- H_2O$), 325 ($M + H^+ - 129$ (Glu) $- 2\,H_2O$), 308 (GSH + H^+).

8a. HPLC retention time 16.6 min; UV: λ_{max} 313 nm; ESI(−)-MS/MS: *m/z* 452 ($M - H^+$), 434 ($M - H^+ - H_2O$), 418 ($M - H^+ - H_2S$), 408 ($M - H^+ - CO_2$), 390 ($M - H^+ - H_2O - CO_2$), 374 ($M - H^+ - H_2S - CO_2$), 356 ($M - H^+ - H_2O - H_2S - CO_2$); ESI(+)-MS/MS: *m/z* 454 ($M + H^+$), 436 ($M + H^+ - H_2O$), 379 ($M + H^+ -$ Gly), 361 ($M + H^+ -$ Gly $- H_2O$), 356 ($M + 2\,H^+ - COCH_2CH_2COCH_3^+$), 308 ($M + H^+ -$ Gly $- CH_2CH_2COCH_3$), 281 ($M + 2\,H^+ -$ Gly $- COCH_2CH_2COCH_3^+$); ^{1}H NMR (D_2O, 500 MHz): δ 7.77 (s, 1H, 2′-H), 6.26 (d, $J = 10.9$ Hz, 1H, 5′-H), 4.42 (t, $J = 4.7$ Hz, 1H, Glu α-CH), 3.94 (s, 2H, Gly α-CH_2), 3.19 (dd, $J = 14.5$, 5.0 Hz, 1H, Cys β-CH_a), 3.02 (d, $J = 15$ Hz, 1H, Cys β-CH_b), 2.96 (t, $J = 14.1$ Hz, 1H, Glu γ-CH_a), 2.91−2.86 (m, 4H, 2-CH_2 and 3-CH_2), 2.61 (dd, $J = 15.5$, 7.5 Hz, 1H, Glu γ-CH_b), 2.43−2.37 (m, 1H, Glu β-CH_a), 2.26 (s, 3H, 5-CH_3), 2.09 (td, $J = 12.9$, 5.5 Hz, 1H, Glu β-CH_b); the signals corresponding to 4′-H and Cys α-CH overlapped with the D_2O peak.

8b: HPLC retention time 17.2 min; UV: λ_{max} 303 nm; ESI(−)-MS/MS: *m/z* 452 ($M - H^+$), 434 ($M - H^+ - H_2O$), 418 ($M - H^+ - H_2S$), 408 ($M - H^+ - CO_2$), 390 ($M - H^+ - H_2O - CO_2$), 374 ($M - H^+ - H_2S - CO_2$), 364 ($M - H^+ - 2\,CO_2$), 356 ($M - H^+ - H_2O - H_2S - CO_2$), 300 ($M - H^+ - H_2S - CO_2 -$ Gly); ESI(+)-MS/MS: *m/z* 454 ($M + H^+$), 436 ($M + H^+ - H_2O$), 379 ($M + H^+ -$ Gly), 361 ($M + H^+ -$ Gly $- H_2O$), 356 ($M + 2\,H^+ - COCH_2CH_2COCH_3^+$), 308 ($M + H^+ -$ Gly $- CH_2CH_2COCH_3$), 281 ($M + 2\,H^+ -$ Gly $- COCH_2CH_2COCH_3^+$). ^{1}H NMR (D_2O, 300 MHz): δ 7.61 (s, 1H, 2′-H), 5.97 (d, $J = 9.3$ Hz, 1H, 5′-H), 2.24 (s, 3H, 5-CH_3); the rest of the signals were not well resolved.

9. HPLC retention time 18.7 min; UV: λ_{max} 248 and 263 nm; ESI-(−)MS/MS: *m/z* 452 ($M - H^+$), 434 ($M - H^+ - H_2O$), 408 ($M - H^+ - CO_2$), 390 ($M - H^+ - H_2O - CO_2$), 364 ($M - H^+ - 2\,CO_2$), 333 ($M - H^+ - CO_2 -$ Gly), 185 (γ-Glu-Cys $-$ CH_7NO_2); ESI(+)-MS/MS: *m/z* 454 ($M + H^+$), 436 ($M + H^+ - H_2O$), 308 ($M + H^+ -$ Gly $- CH_2CH_2COCH_3$).

10a. HPLC retention time 19.3 min; UV: λ_{max} 245 and 277 nm. HPLC reanalysis showed that most of **10a** had rearranged to **10b** after isolation.

10b. HPLC retention time 19.9 min; UV: λ_{max} 240 and 277 nm; ESI-(−)MS/MS: *m/z* 452 ($M - H^+$), 434 ($M - H^+ - H_2O$), 408 ($M - H^+ - CO_2$), 390 ($M - H^+ - H_2O - CO_2$); ESI(+)-MS/MS: *m/z* 454 ($M + H^+$), 436 ($M + H^+ - H_2O$), 379 ($M + H^+ -$ Gly), 361 ($M + H^+ - H_2O -$ Gly), 356 ($M + 2\,H^+ - COCH_2CH_2COCH_3^+$), 281 ($M + 2\,H^+ -$ Gly $- COCH_2CH_2COCH_3^+$); ^{1}H NMR (D_2O, 500 MHz): δ 7.91 (s, 1H, 2′-H), 7.04 (s, 1H, 4′-H), 5.28 (dd, $J = 13.5$, 4.0 Hz, 1H, Glu α-CH), 3.91 (AB quartet, $J = 18.0$ Hz, 2H, Gly α-CH_2), 3.52 (dd, $J = 14.8$, 3.1 Hz, 1H, Cys β-CH_a), 3.25−3.14 (m, 2H, 2-CH_2), 3.02−2.93 (m, 3H, Cys β-CH_b and 3-CH_2), 2.70 (tt, $J = 12.5$, 4.7 Hz, 1H, Glu β-CH_a), 2.61 (dd, $J = 13.3$, 6.3 Hz, 1H, Glu γ-CH_a), 2.53 (td, $J = 13.3$, 4.7 Hz, 1H, Glu β-CH_b), 2.30 (s, 3H, 5-CH_3), 2.10 (td, $J = 12.5$, 6.3 Hz, 1H, Glu γ-CH_b); the signal corresponding to Cys α-CH overlapped with the D_2O peak.

Several minor products (**11**−**13**) that did not have the distinctive UV absorption maximum above 260 nm were also isolated by HPLC. Compd **11** was present in the 17.9−18.4 min fraction, and **12** and **9** were isolated in one fraction at approximately 18.7 min. The ESI(−)-MS/MS of **11** and **12** were identical: *m/z* 759 ($M - H^+$), 741 ($M - H^+ - H_2O$), 630 ($M - H^+ - 129$ (Glu)), 486 ($M - H^+ - 273$ (GSH $- H_2S$)), 468 ($M - H^+ - 273$ (GSH $- H_2S$) $- H_2O$). ESI(+)-MS/MS: *m/z* 761 ($M + H^+$), 743 ($M + H^+ - H_2O$), 686 ($M + H^+ -$ Gly), 632 ($M + H^+ - 129$ (Glu)), 614 ($M + H^+ - 129$ (Glu) $- H_2O$). **13** was isolated along with **10a** with an approximate HPLC retention time at 19.3 min; ESI(−)-MS/MS: *m/z* 731 ($M - H^+$), 713 ($M - H^+ - H_2O$), 679 ($M - H^+ - H_2O - H_2S$), 602 ($M - H^+ - 129$ (Glu)), 458 ($M - H^+ - 273$ (GSH $- H_2S$)); ESI(+)-MS/MS: *m/z* 733 ($M + H^+$), 715 ($M +$

Scheme 1. Gly, AcCys, and Cys Adducts Identified in the Microsomal Incubations of IPN

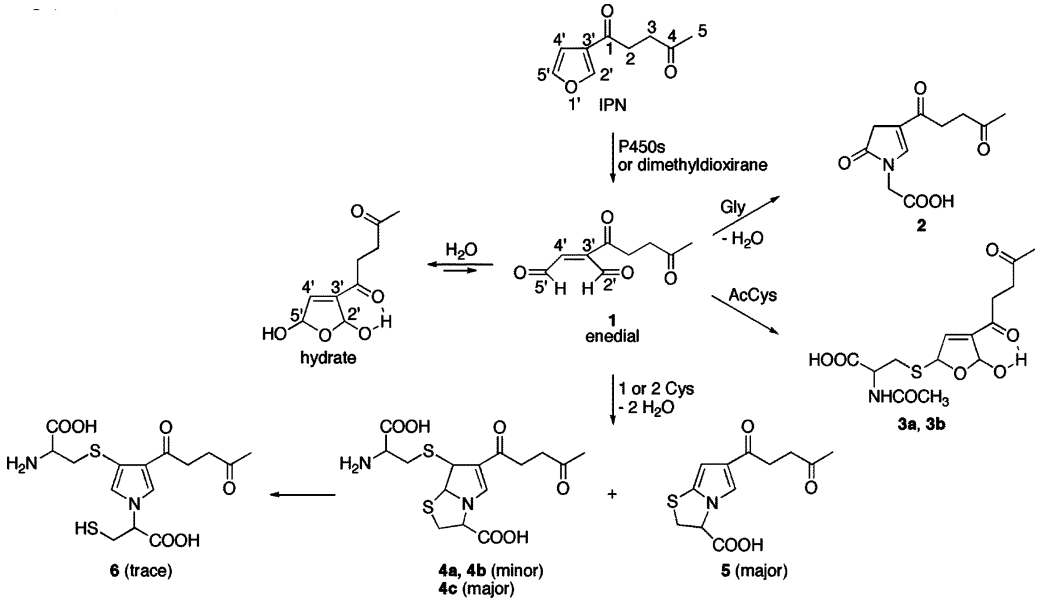

$H^+ - H_2O$), 658 ($M + H^+ -$ Gly), 604 ($M + H^+ -$ 129 (Glu)), 586 ($M + H^+ -$ 129 (Glu) $- H_2O$).

Incubation of 4-IPO with Rat Liver Microsomes and NADPH in the Presence of GSH. Incubations of 4-IPO (1 mM) and GSH (5 mM) with male F344 rat liver microsomes (2 mg protein/mL) were conducted under the same conditions as IPN. The incubation took place at 37 °C in capped vials for 3 h. Control experiments omitting either $NADP^+$ or GSH were included. HPLC-UV analysis of the incubation mixture revealed the formation of IPN, **8a**−**b** and **10b** along with new products (**14**−**17**) (Figure 2C and D). These peaks were collected along with fractions between peaks so as to include the most products. The products observed by HPLC-UV and also **9**, **11**, and **12** and other new products (**18**−**20**) were characterized by ESI-MS. The peak eluting at 12.4 min (Figure 2B and D) was also observed in a control experiment including only GSH, the NADPH regenerating system, and the buffer and, therefore, is not a metabolite of IPN or 4-IPO.

14. HPLC retention time 15.1 min; UV: λ_{max} 312 nm; ESI(−)-MS/MS: *m/z* 454 ($M - H^+$), 436 ($M - H^+ - H_2O$), 420 ($M - H^+ - H_2S$), 410 ($M - H^+ - CO_2$), 392 ($M - H^+ - H_2O - CO_2$), 376 ($M - H^+ - H_2S - CO_2$), 358 ($M - H^+ - H_2O - H_2S - CO_2$); ESI(+)-MS/MS: *m/z* 456 ($M + H^+$), 438 ($M + H^+ - H_2O$), 420 ($M + H^+ - 2\ H_2O$), 381 ($M + H^+ -$ Gly), 363 ($M + H^+ -$ Gly $- H_2O$), 278 ($M + H^+ -$ Cys-Gly).

The formation of **15** required 4-IPO, rat liver microsomes, and the NADPH regenerating system but not GSH. Its properties were as follows: HPLC retention time 15.4 min; UV: λ_{max} 214 and 257 nm; ESI(−)-MS/MS: *m/z* 788 ($M - H^+$), 770 ($M - H^+ - H_2O$), 690 ($M - H^+ - H_3PO_4$), 653 ($M - H^+ -$ adenine), 620 ($M - H^+ -$ 4-ipomeanol), 441 ($M - H^+ -$ adenosine 2′-monophosphate), 426 (adenosine 2′, 5′-diphosphate), 408 (adenosine 2′,5′-diphosphate $- H_2O$).

16. HPLC retention time was 17.5 min; UV: λ_{max} 250 and 262 nm; ESI(−)-MS/MS: *m/z* 454 ($M - H^+$), 436 ($M - H^+ - H_2O$), 410 ($M - H^+ - CO_2$), 392 ($M - H^+ - H_2O - CO_2$), 366 ($M - H^+ - 2\ CO_2$), 335 ($M - H^+ - CO_2 -$ Gly), 185 (γ-Glu-Cys $- CH_7NO_2$).

17. HPLC retention time was 18.7 min; UV: λ_{max} 242 and 277 nm. This product was isolated from HPLC along with DIOL (retention time at 19.0 min, UV: λ_{max} 212 nm). The other spectral properties of **17** were as follows: ESI(−)-MS/MS: *m/z* 454 ($M - H^+$), 436 ($M - H^+ - H_2O$), 410 ($M - H^+ - CO_2$), 310 ($M - CO_2 - COCH_2CH_2CHOHCH_3^+$); ESI(+)-MS/MS: *m/z* 438 ($M + H^+ - H_2O$), 420 ($M + H^+ - 2\ H_2O$), 363 ($M + H^+ - H_2O -$ Gly), 356 ($M + 2\ H^+ - COCH_2CH_2CHOHCH_3^+$), 335 ($M + H^+ - H_2O -$ $HCONHCH_2COOH$), 281 ($M + 2\ H^+ -$ Gly $- COCH_2$-$CH_2CHOHCH_3^+$); ^{1}H NMR (D_2O, 300 MHz): δ 7.85 (s, 1H, 2′-H), 7.00 (s, 1H, 4′-H), 5.19 (dd, $J = 11.7$, 4.2 Hz, 1H, Glu -CH), 1.19 (d, $J = 6.3$ Hz, 3H, 5-CH_3); the other signals were not resolved or overlapped with the signals of DIOL.

18. Approximate HPLC retention time was 17.3 min; ESI(−)-MS/MS: *m/z* 761 ($M - H^+$), 743 ($M - H^+ - H_2O$), 709 ($M - H^+ - H_2O - H_2S$), 632 ($M - H^+ -$ 129 (Glu)), 488 ($M - H^+ -$ 273 (GSH $- H_2S$)).

19: approximate HPLC retention time was 17.9 min; ESI(−)-MS/MS: *m/z* 761 ($M - H^+$), 743 ($M - H^+ - H_2O$), 709 ($M - H^+ - H_2O - H_2S$), 632 ($M - H^+ -$ 129 (Glu)), 488 ($M - H^+ -$ 273 (GSH $- H_2S$)), 470 ($M - H^+ -$ 273 (GSH $- H_2S$) $- H_2O$). Compd **20** was isolated along with **17**. ESI(−)-MS/MS of **20**: *m/z* 733 ($M - H^+$), 715 ($M - H^+ - H_2O$), 681 ($M - H^+ - H_2O - H_2S$), 604 ($M - H^+ -$ 129 (Glu)), 460 ($M - H^+ -$ 273 (GSH $- H_2S$)).

Incubation of DIOL with Rat Liver Microsomes and NADPH in the Presence of GSH. Incubations of DIOL (1 mM) and GSH (5 mM) with male F344 rat liver microsomes (2 mg protein/mL) were conducted under the same conditions as IPN. The incubation took place at 37 °C in capped vials for 3 h. Control experiments omitting $NADP^+$ were included. HPLC analysis of the incubation mixture revealed the formation of trace amounts of 4-IPO and an unknown product eluting at 17.4 min that was not characterized.

Results

Oxidation of IPN by Dimethyldioxirane-d_6. The oxidation of IPN by dimethyldioxirane-d_6 was followed by ^{1}H NMR spectroscopy. The formation of enedial **1** (Scheme 1) was indicated by the appearance of signals for two aldehyde protons at 10.25 ppm (5′-H) and 10.21 ppm (2′-H) and an olefinic proton at 6.95 ppm (4′-H). The signals for the aliphatic protons overlapped with the signals of IPN. The 4′-H has a ^3J coupling (6 Hz) with 5′-H and a long range ^4J coupling (1.7 Hz) with 2′-H. A hydrate of **1** that existed as a mixture of cis and trans isomers was also detected in the ^{1}H NMR spectrum (Scheme 1). Endial **1** was detectable in the reaction mixture for the first 2 h. After 2 h, **1** was not detected, but the hydrate was still detectable.

Incubations of IPN with Rat Liver Microsomes and NADPH in the Presence of Gly, AcCys, Cys, or GSH. All incubation mixtures were analyzed by HPLC with UV detection from 190 to 350 nm. IPN eluted at 23.7 min. 4-IPO (retention

time at 22.6 min), generated from the reduction of IPN, was observed in all incubations. The other products were isolated by HPLC and characterized by MS and/or ^{1}H NMR spectroscopy. The spectral data of these products are listed in Experimental Procedures, and the structural assignments are described below.

1. Gly. One product eluting at 14.5 min (**2**) had a UV maximum at 295 nm and a molecular weight (MW) of 239. The MW is equivalent to IPN + [O] + Gly minus one H_2O. The MS and ^{1}H NMR spectrum indicate that the side chain of IPN remains intact in the product; therefore, the microsomal oxidation occurred in the furan moiety of IPN. The intense UV absorption maximum at 295 nm in the metabolite can only be due to a β-aminoenone (COC═CHNR$_2$) from the reaction of the enedial with Gly. Using Woodward's Rules to estimate the UV absorption maxima of enones, only β-amino and β-thioenones are predicted to have maxima in the 290+ nm range. NADPH, for example, contains a similar β-amino-α,β-unsaturated amide that accounts for the observed UV maximum at 340 nm. One ^{1}H NMR signal at 7.93 ppm as a singlet confirms the presence of the olefin proton 2′-H in the product. The chemical shift of 2′-H in **2** is upfield compared with that of 2′-H in IPN (8.38 ppm in D_2O), consistent with the replacement of the furyl O with an N. Product **2** is assigned as a 2′-pyrrolin-5′-one (Scheme 1). The 4′-CH$_2$ resonance at 3.37 ppm as a singlet is consistent with the assigned structure.

2. AcCys. Two products (**3a** and **3b**) eluting at 16.3 and 16.4 min were observed. They had a similar UV maximum at 263 nm. An analysis of the MS of **3a** and **3b** indicated that they had a MW of 345, corresponding to a 1:1 adduct of enedial **1** and AcCys. Characterization of the adducts from the conjugation of **1** with Cys or GSH indicated that the addition of thiols to **1** occurred at the 4′- or 5′- but not the 2′-positions (vide infra). AcCys is expected to add to **1** at either the 4′- or the 5′-position, but only the addition at the 5′-aldehyde would give an enone product with a UV maximum at 263 nm. The adducts **3a**−**b** are tentatively assigned as two diastereomeric 2′,5′-dihydro-2′-hydroxyfurans (Scheme 1).

3. Cys. Two minor products eluting at 15.7 min (**4a**) and 16.3 min (**4b**) and two major products eluting at 16.7 min (**4c**) and 27.6 min (**5**) were observed. The UV spectra of **4a**−**c** were similar, with a single maximum around 300 nm. An analysis of the MS indicated that **4a**−**c** all had a MW of 388 with similar MS/MS fragmentation patterns corresponding to an adduct between enedial **1** and two Cys molecules minus two H_2O molecules. Only **4c** was abundant enough for a ^{1}H NMR spectrum. The NMR spectrum contained two one-proton singlets at 7.61 ppm (2′-H) and 5.35 ppm (5′-H). Previous studies with furan and 4-IPO have shown that the enedial metabolites form pyrrole adducts with reactants containing a primary amine and a thiol such as GSH (*9*, *13*, *14*). Compd **1** incorporated two Cys molecules to give **4a**−**c**, but the UV absorption and the NMR spectrum of **4c** suggest that the structures of **4a**−**c** are similar to **2** rather than those of the expected pyrroles. The single UV maximum of **4c** at 304 nm and the olefin proton at 7.61 ppm are in agreement with an enone substituted with a β-amino group (COC═CHNR$_2$), but the 5.35 ppm singlet is not what would be expected for a pyrrole proton. The chemical shift is consistent with a proton on a carbon substituted with one N and one S, as the proposed structure for **4c** shows in Scheme 1. The signal corresponding to 4′-H is likely obscured by the D_2O peak. The structure consists of a bicyclic 2-pyrroline with the thiols of two Cys molecules substituted at the 4′- and 5′-positions to form two chiral centers. The 5.35 ppm singlet assigned to the 5′-H of **4c** indicates that coupling between 4′-H and 5′-H is near zero. GMMX-calculated coupling constants of vicinal protons in a saturated cyclopentane ring have been published: *J* cis is up to 11.5 Hz and never below 5 Hz, whereas *J* trans varies from 0.3 to 13 Hz (*22*). The experimental data from more than 30 saturated cyclopentanes generally follow this trend (*22*). The 4′-H and 5′-H in **4c** are assigned as trans to each other on the basis of this observation. **4a** and **4b** were not abundant enough to obtain ^{1}H NMR spectra, and they are tentatively assigned as diastereomers of **4c** (Scheme 1).

An analysis of the MS of **5** indicated a MW of 267, corresponding to a 1:1 adduct between enedial **1** and Cys followed by loss of two H_2O moecules. Compd **5** had UV maxima at 231 (major) and 308 nm. The two maxima are consistent with the UV absorption of a pyrrole molecule in contrast to the single maximum near 300 nm for the β-aminoenones. The ^{1}H NMR spectrum of **5** contained two one-proton singlets at 7.77 ppm and at 6.31 ppm. The singlet at 7.77 ppm is slightly more downfield than that of the olefin proton (2′-H) in **4c** (7.61 ppm), as expected for a pyrrole 2′-CH. The singlet at 6.31 ppm is upfield compared to that of the furyl proton (4′-H) in IPN (6.80 ppm). Compd **5** is assigned as a mono-Cys 5′-S-pyrrole with the singlets at 6.31 and 7.77 ppm assigned to 4′-CH and 2′-CH, respectively, as shown in Scheme 1.

4. GSH. Numerous products with distinctive UV absorption maxima were observed by HPLC (Figure 2A and B). The products can be divided into two groups: one with UV maxima around 250 nm, which includes **7a**−**b**, **9**, **10a**−**b** (Figure 2A), and the other with UV maxima around 300 nm, which includes **8a**−**b** (Figure 2B). The two most polar products (**7a** and **7b**), eluting at 13.6 and 13.7 min, had a similar UV maximum at 262 nm. An analysis of the MS of the mixture of **7a** and **7b** indicates that they had a MW of 489, corresponding to a 1:1 adduct between enedial **1** and GSH. The UV absorption and MS of **7a** and **7b** are similar to those of **3a** and **3b**, indicating adducts of similar structure. Compds **7a** and **7b** are assigned as diastereomeric 2′,5′-dihydro-2′-hydroxyfurans (Scheme 2). After **7a** and **7b** were stored at −20 °C for some time, HPLC reanalysis showed that they had converted to **10a** and **10b** in a 1:1 ratio.

Two major products (**8a** and **8b**), eluting at 16.6 and 17.2 min, had distinctive single UV maxima at 313 and 303 nm, respectively. An analysis of the MS indicated both **8a** and **8b** had MWs of 453 with a similar MS/MS fragmentation, corresponding to a 1:1 adduct between enedial **1** and GSH minus two H_2O molecules. The ^{1}H NMR spectrum of **8a** contained a one-proton singlet at 7.77 ppm and a one-proton doublet at 6.26 ppm (J = 10.9 Hz). A 2D ^{1}H-^{1}H DQF COSY NMR experiment indicated that the 6.26 ppm proton coupled with a peak obscured by the D_2O peak. The ^{1}H NMR spectrum of **8b** contained a one-proton singlet (2′-H) at 7.61 ppm and a one-proton doublet (J = 9.3 Hz, 5′-H) at 5.97 ppm. The single UV maximum at 313 or 303 nm and the olefin proton singlet (2′-H) observed at 7.77 or 7.61 ppm are in agreement with an enone substituted with a β-amino group (COC═CHNR$_2$). The chemical shifts of 5′-H in **8a** and **8b** are consistent with the protons on sp^3 carbons substituted with one N and one O, and 4′-H and 5′-H are coupled to each other with the coupling constant around 10 Hz. The UV and NMR spectra demonstrate that **8a** and **8b** are structurally similar to the bicyclic 2′-pyrroline adducts **4a**−**c** except that the Cys of GSH is substituted at the 4′-position, and the Glu α-carboxylic acid of GSH is substituted at the 5′-position to form tricyclic 2′-pyrrolines, as shown Scheme 2. There are two chiral centers at 4′-C and 5′-C, and in theory, there should

Scheme 2. GSH Adducts Identified in the Microsomal Incubation of IPN

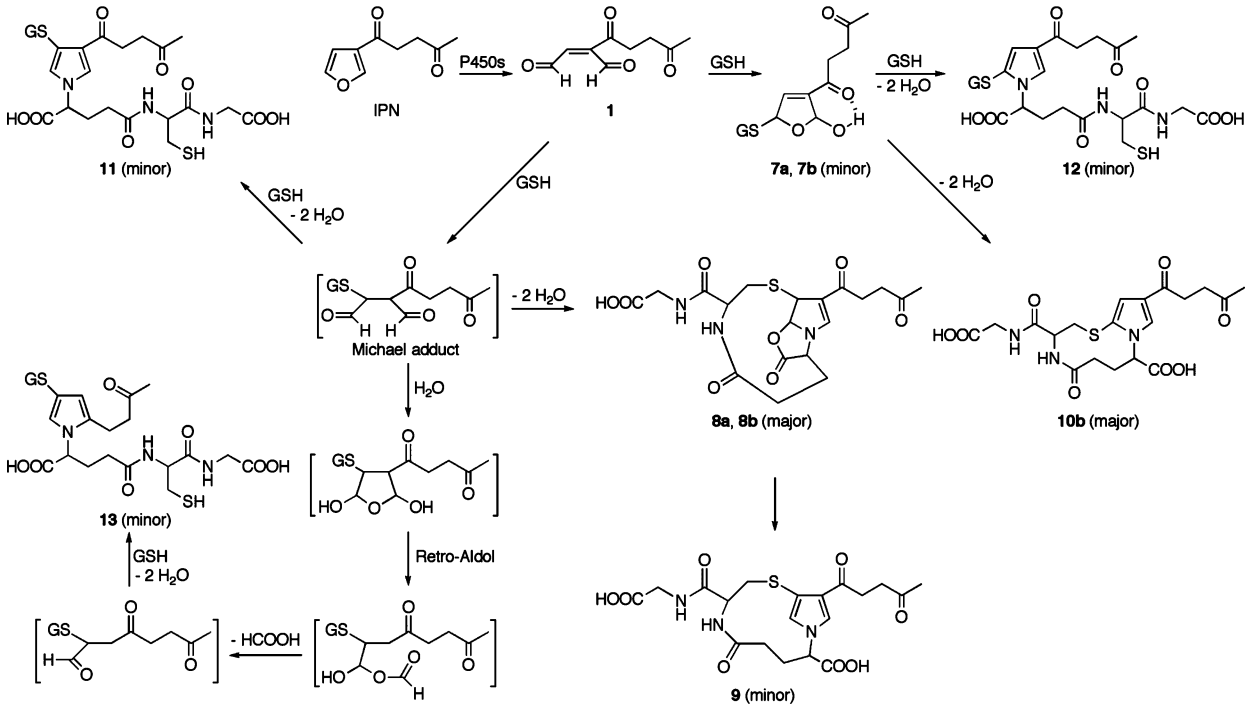

be four diastereomers. Two isomers, **8a** and **8b**, were observed, but the cis−trans relationship of 4′-H and 5′-H cannot be decided on the basis of the coupling constants of 5′-H. As stated earlier, both vicinal cis and trans protons in a saturated cyclopentane ring can have coupling constants up to 11.5−13 Hz (*22*).

A portion of **8a** and **8b** rearranged to **9** eluting at 18.7 min upon storage. Compd **9** had two UV maxima at 248 and 263 nm and a MW of 453, the same MW as that of **8a** and **8b**. The UV absorption of **9** indicates that it is likely a pyrrole. An attempt to obtain a ^{1}H NMR spectrum of **9** was not successful because it partially degraded during HPLC isolation. Compd **9** is tentatively assigned as a 4′-S-pyrrole adduct shown in Scheme 2.

The UV absorption of one minor product (**10a**, UV: λ_{max} 245 and 277 nm) eluting at 19.3 min and one major product (**10b**, UV: λ_{max} 240 and 277 nm) eluting at 19.9 min indicates that they are likely to be pyrroles. Most of **10a** rearranged to **10b** after collection from HPLC. The MS showed that **10b** had a MW of 453, the same MW as that of **8a**−**b** and **9**. The ^{1}H NMR spectrum of **10b** showed two singlets at 7.91 and 7.04 ppm, representing two pyrrole protons. The singlet at 7.91 ppm can be easily assigned to 2′-H, but the signal at 7.04 ppm can be assigned to either 4′-H or 5′-H. In order to determine the position of the S-substitution, a 2D TROESY NMR experiment of **10b** was carried out. The pyrrole proton at 7.91 ppm showed proximity to 2-CH_2 on the IPN side chain and the protons on Glu (β-CH_b at 2.53 ppm and γ-CH_b at 2.10 ppm), in agreement with the 2′-H assignment. The other pyrrole proton at 7.04 ppm showed proximity to 2-CH_2 on the IPN side chain and the proton on the Cys (β-CH_b at approximately 3 ppm) but had no interactions with the protons on Glu. These interactions indicated that the proton at 7.04 ppm is positioned between the IPN side chain and the Cys chain and can only be assigned to 4′-H. A 2D ^{1}H-^{13}C HSQC NMR experiment observed the chemical shifts of the carbons attached to the assigned 2′-H and 4′-H at 131 and 120 ppm, respectively, in agreement with the predicted chemical shifts for 2′-C and 4′-C. Compd **10b** is assigned as a 5′-S-pyrrole adduct as shown by its structure in Scheme 2. After storage at −20 °C for some time, reanalysis of the mixture of **7a**−**b** by HPLC showed that they had converted to **10a** and **10b** in a 1:1 ratio. This observation not only confirms that the S-substitution of **10b** is at 5′-C but also demonstrates that the cyclization of **7a** and **7b** initially gives **10a**, which then rearranges to **10b**. The structure of **10a** is not known at this point. The rearrangement of **8a** and **8b** gave rise to **9** instead of **10b**, more indirect evidence to support the structure of **10b**.

Several minor GSH adducts were isolated along with the major adducts and were subsequently characterized by MS (Scheme 2). Two adducts eluting around 17.9−18.4 min (**11**) and 18.7 min (**12**) had MWs of 760, consistent with the conjugation of **1** with two GSH molecules minus 2 H_2O molecules. They are tentatively assigned as bis-GSH 4′-S- and 5′-S-pyrroles **11** and **12** as shown in Scheme 2. Another adduct, **13**, had a MW of 732, 28 Da, a C═O group, less than those of the bis-GSH pyrrole addcuts **11** and **12**. Compd **13** is tentatively assigned as a bis-GSH pyrrole adduct (Scheme 2).

Incubation of 4-IPO with Rat Liver Microsomes and NADPH in the Presence of GSH. HPLC-UV analysis of the incubation mixture revealed the formation of IPN, **8a**−**b**, and **10b** along with new products (**14**−**17**) (Figure 2C and D). These products can be divided into two groups: one with a UV maximum around 250 nm, which includes **15**−**17** and **10b** (Figure 2C), and the other with a UV maximum around 300 nm, which includes **14** and **8a**−**b** (Figure 2D). There was a peak eluting at 19.0 min with a UV maximum at 212 nm. The product was characterized as a DIOL on the basis of a comparison of its HPLC retention time, UV maximum, and ^{1}H NMR data with those of synthetic DIOL diastereomers (HPLC retention times at 18.5 and 19.0 min). Other products, including **9**, **11**, and **12**, and new products (**18**−**20**) were also isolated by HPLC and detected by MS.

Compd **15** had a MW of 789, and the ESI(-)-MS/MS showed that 4-IPO and adenosine-2′,5′-diphosphate were parts of the molecule. The UV maxima of **15** at 214 and 257 nm are similar to those of 4-IPO and adenine. The formation of **15** required 4-IPO, rat liver microsomes, and the NADPH regenerating

Scheme 3. GSH Adducts Identified in the Microsomal Incubation of 4-IPO

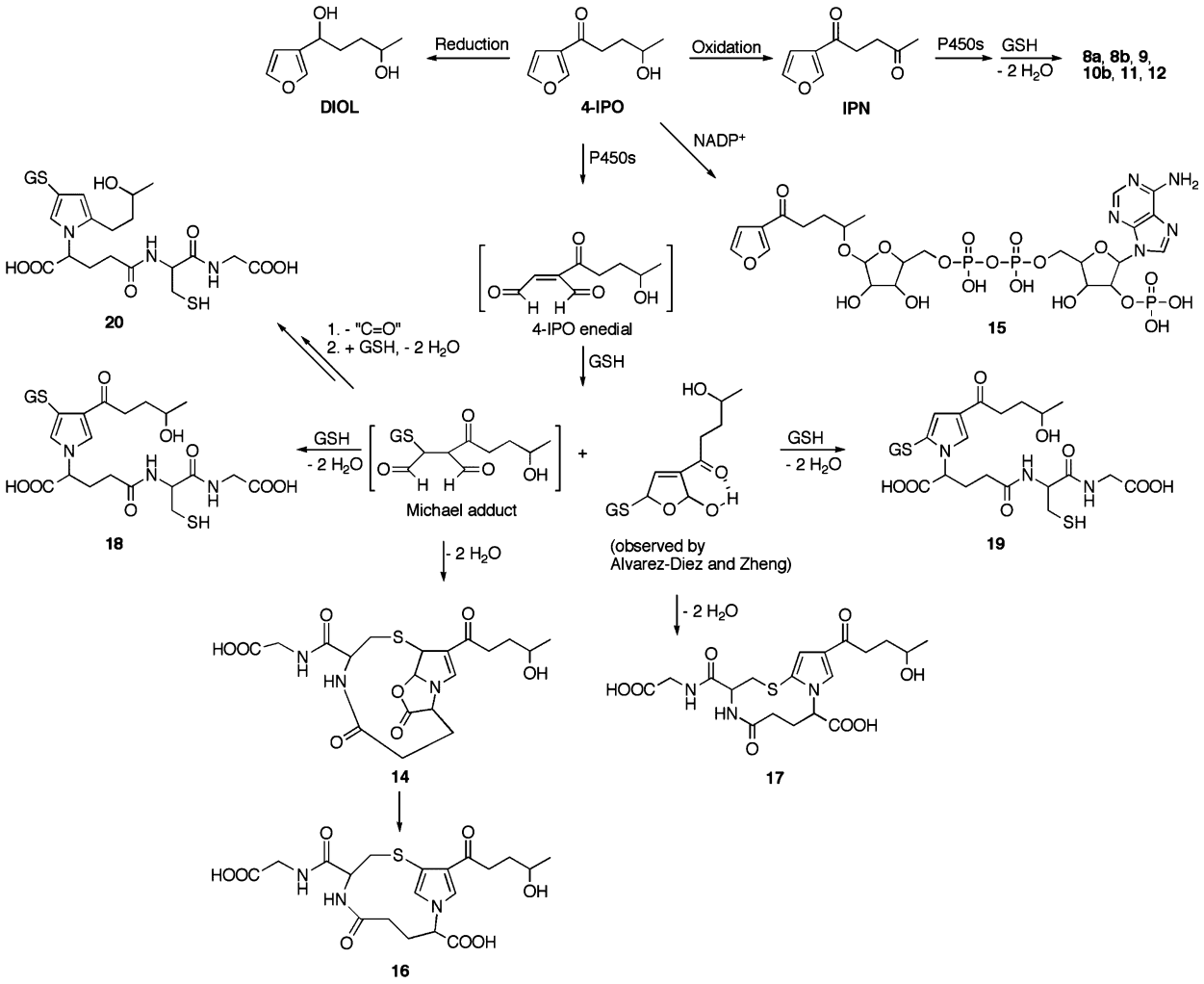

system but not GSH. The displacement of the nicotinamide (121) of $NADP^+$ (743) by 4-IPO (167) would give **15** (Scheme 3). Both the MS/MS fragmentation and the UV absorption support the assigned structure.

Both **16** and **17** have a MW of 455, corresponding to a 1:1 adduct between the enedial metabolite of 4-IPO and GSH minus two H_2O molecules. UV absorption of **16** (UV: λ_{max} 250 and 262 nm) and **17** (UV: λ_{max} 242 and 277 nm) indicates that they are likely pyrroles. The ^1H NMR spectrum of **17** clearly showed two pyrrole protons at 7.85 ppm (2′-CH) as a singlet and at 7.00 ppm (4′-CH) as a singlet. Compds **16** and **17** had UV absorptions similar to those of **9** and **10b**, respectively, and MWs 2 Da higher than those of **9** and **10b**. The chemical shifts of 2′-H and 4′-H in **17** are 0.06 and 0.04 ppm, respectively, upfield than those in **10b**. Compds **16** and **17** were assigned as mono-GSH 4′-S− and 5′-S-pyrroles (Scheme 3). Both **18** and **19** had a MW of 762, consistent with the conjugation of the enedial metabolite of 4-IPO with two GSH molecules minus 2 H_2O moelcules. The MWs are 2Da higher than those of **11** and **12**. The UV absorption of **18** and **19** were not distinctive. Compds **18** and **19** are tentatively assigned as bis-GSH 4′-S- and 5′-S-pyrroles (Scheme 3).

Compd **14** had a UV maximum at 312 nm and a MW of 455, the same as that of **16** and **17**. The structure of **14** is likely similar to those of **8a**−**b**, except for the side chain having a 4-OH instead of a 4-C═O (Scheme 3). Compd **20** was isolated along with **17** and, subsequently, detected by mass spectrometry. Compd **20** had a MW of 734, 28 Da, a C═O group, less than those of the bis-GSH pyrrole adducts **18** and **19** and 2 Da higher than that of **13**. Compd **20** is tentatively assigned as the bis-GSH pyrrole adduct (Scheme 3).

Discussion

While the metabolic activation of 4-IPO by cytochromes P450 seems well established, only recently have metabolites derived from the reactive intermediate been characterized. However, the multicenter reactivity of the enedial intermediate has not been evident in metabolites identified in previous studies (*8, 9*). These recent studies focused on 4-IPO metabolism as did our initial studies. The yield of products from microsomal incubations of 4-IPO was limited, apparently because oxidizing equivalents were being consumed by oxidation of the alcohol moiety in 4-IPO to a ketone. By starting with IPN, this pathway was not available, and higher yields of metabolites were produced. The chemical oxidation of 4-IPO by dimethyldioxarane also led to oxidation of the alcohol and reduced the yield of oxidized furan products (data not shown).

The chemical oxidation of IPN by dimethyldioxirane to enedial **1** and subsequent reaction with H_2O to form a hydrate, was observed using NMR spectroscopy. *cis*-2-Butene-1,4-dial from the oxidation of furan forms a stable hydrate (*12*), and likewise, the hydrate of enedial **1** is more stable than **1**. Although metabolic schemes for furans often include epoxides, furan epoxides have been detected only at 0 °C or lower temperatures (*23*−*25*). In several studies, only enedials were observed at room

Scheme 4. Proposed Mechanisms for the Formation of 8a−b (A) and 4a−c (B)

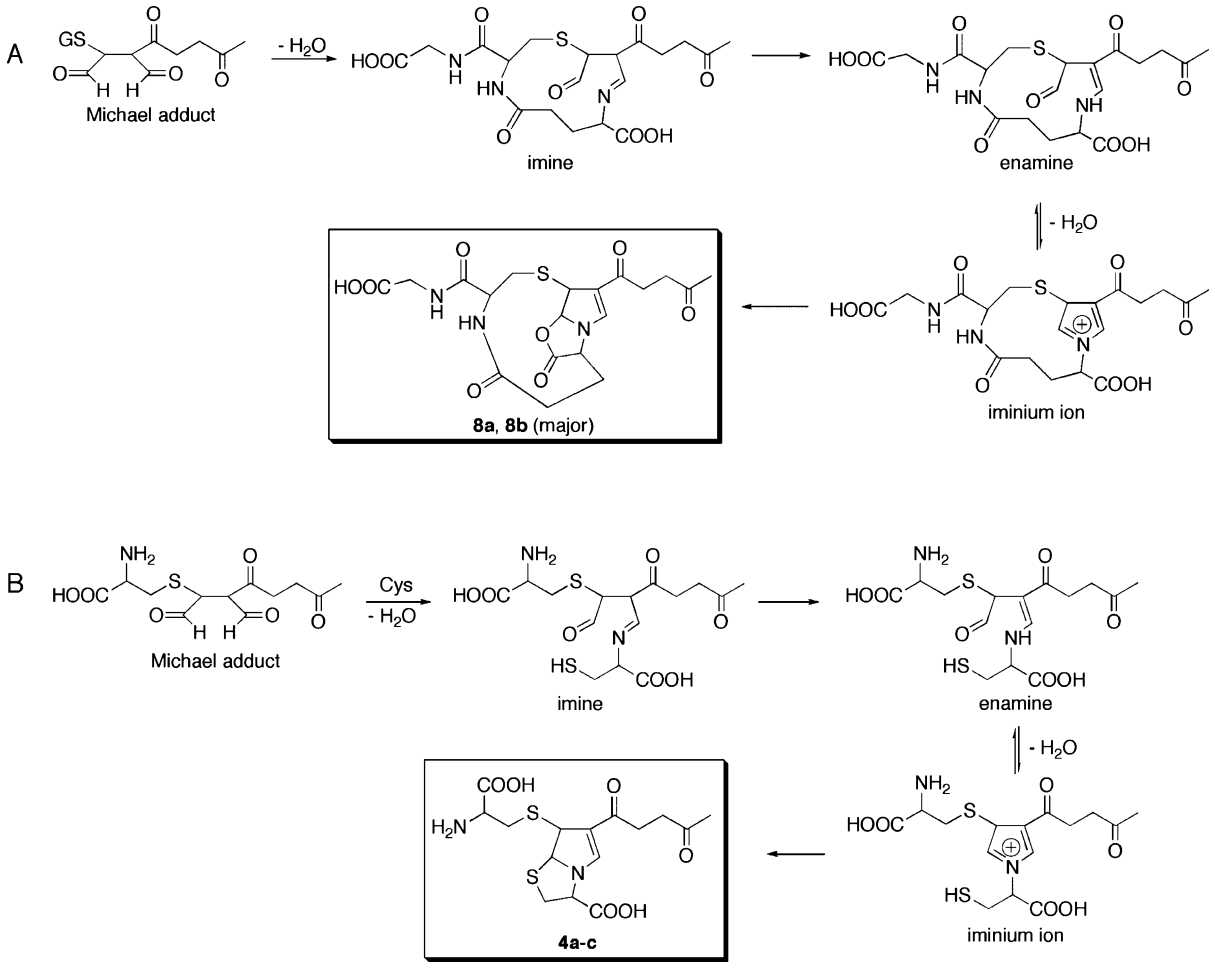

temperature from the chemical oxidation of furans (*12*, *24*, *25*), and the present study confirms these results. Furans substituted with an electron-withdrawing group in the 3-position have generally been resistant to oxidation by reagents that are electrophilic in nature, for example, peracids (*26*). Dimethyldioxirane is considered to be nucleophilic (*21*). If that is true, then the keto functionality at the 3′-position reduces electron density at 2′-C and may actually facilitate oxidation by this reagent. However, compared to the complete oxidation of furan by dimethyldioxirane to *cis*-2-butene-1,4-dial within 30 min (*12*), the oxidation of IPN by dimethyldioxirane to enedial **1** was incomplete, suggesting that the electron-withdrawing carbonyl group may still slow the oxidation even though the oxidant has some nucleophilic properties. The nucleophilic attack at 2′-C may be slowed by steric interference, the reaction may be inherently slower, or the double bonds in furan are identical, and therefore, a statistical factor may also be involved there. Demonstration of adduct formation was not possible in the chemical oxidation studies because the usual nuclephiles were destroyed by the excess oxidizing equivalents.

Investigation of microsomal oxidation of IPN began with simple nucleophiles and progressed to more complex ones. The assignment of structure at each level of complexity was aided by the information provided by earlier, simpler products. 2′-Pyrrolin-5′-one adduct **2** was identified in the rat liver microsomal incubation of IPN containing NADPH and Gly. The characterization of this 2′-pyrrolin-5′-one adduct establishes that IPN is metabolized by rat liver microsomes to enedial **1**. Primary amines are known to conjugate with *cis*-2-butene-1,4-dial to give a mixture of 3-pyrrolin-2-one and 4-pyrrolin-2-one or with the ketoenal metabolite of menthofuran to give a 3-pyrrolin-2-one (*13*, *16*).

The 1,2-addition of AcCys or GSH to the 5′-aldehyde of the enedial **1** gave isolable dihydrohydroxyfuran adducts **3a**−**b** and **7a**−**b**. The intramolecular H bonding between the 2′-OH group and 3′-keto group probably stabilizes these adducts. Four biliary metabolites of 4-IPO with MWs 2 Da higher than those of **7a**−**b** were detected in rats (*8*). Several aldehyde-containing structures were proposed in ref *8*, but we suspect that two metabolites are likely analogues to **7a**−**b** as the structures show in Scheme 3. Alvarez-Diez and Zheng (*8*) and the present work demonstrate that both enedial metabolites of IPN and 4-IPO conjugate with thiols to give persistent dihydrohydroxyfuran adducts. These dihydrohydroxyfuran adducts are capable of reacting with an amine to form cross-linking pyrrole adducts and, therefore, might play roles related to the toxicity of IPN and 4-IPO. Metabolism of menthofuran in rats gave a biliary metabolite, 2-(glutathion-*S*-yl)menthofuran, from the reaction of the ketoenal metabolite with GSH followed by dehydration of the hemiketal intermediate (*15*). The hemiacetal groups in **3a**−**b** and **7a**−**b** do not dehydrate to form furans. Instead, if the trapping agents also contained amino groups, then the dihydrohydroxyfuran metabolites would be subject to the addition of the amine followed by dehydration to give 5′-*S*-pyrrole adducts. That is, cyclization of **7a**−**b** gave **10a** and **10b,** and the addition of a second GSH to **7a**−**b** formed **12**. The 5′-*S*-pyrrole adduct **5** was a major product in the rat liver microsomal incubation of IPN, NADPH, and Cys. The dihydrohydroxyfuran intermediates from the conjugation of the Cys thiol with the 5′-aldehyde of **1** were too short-lived for observation.

The 1,4-addition (Michael addition) of Cys or GSH to **1** at the 4-position gave 2-pyrrolines, **4a**−**c** and **8a**−**b**, instead of the expected 4′-*S*-pyrroles. The proposed mechanisms for their formation are shown in Scheme 4. The GSH Michael adduct of **1** yields an imine upon cyclization, which could tautomerize to the corresponding enamine. The enamino aldehyde would be in equilibrium with the corresponding iminium ion, as shown by Castagnoli et al. (*27*) in their study of cyclic tertiary amine oxidation. The addition of Glu α-carboxylic acid to the iminium ion gives **8a**−**b**. The mechanism for the formation of **4a**−**c** is similar. Starting from the Cys Michael adduct of **1**, the intermediate reacts with the amino group in a second Cys molecule to form an imine. Tautomerization of the imine followed by dehydration gives an iminium ion. Addition of the second Cys thiol to the iminium ion gives the products (Scheme 4). The GSH or Cys Michael adducts of **1** shown in Scheme 4 might exist in the incubations, but unlike **3a**−**b** and **7a**−**b**, these Michael adducts could not be observed because of a lack of UV absorption. Similarly, the AcCys Michael adduct of **1**, if it exists, could not be observed because of a lack of UV absorption and a lack of further reactions to give products with UV chromophores. A portion of **8a**−**b** rearranged to the 4′-*S*-pyrrole **9** during storage. The addition of a second GSH to the GSH Michael adduct of **1** and subsequent loss of two H_2O molecules would give **11**. Loss of C═O, as formate, via a retro-aldol condensation followed by the addition of a second GSH and dehydration would give the pyrrole adduct **13** (Scheme 2). No adducts from the conjugation of thiols with the 2′-aldehyde in **1** were observed. Baer et al. (*9*) and this study demonstrate that addition of thiols to the enedial metabolites of 4-IPO and IPN occurred only at the 4′- or 5′- but not 2′-positions, probably due to the fact that 4′-C is β to both a ketone and an aldehyde, which facilitates Michael addition, and 5′-C may be more accessible than 2′-C. The mono-GSH adducts **7a**−**b**, **8a**−**b**, **9** and **10b** were also observed in the rat lung microsomal incubations of IPN (data not shown). The major difference between rat liver and lung microsomal incubations of IPN is that a smaller amount of IPN was reduced to 4-IPO in the lung preparation. The metabolites with the distinct UV maximum around 300 nm such as **2**, **4a**−**c** and **8a**−**b** or their analogues would be good biomarkers for studying the in vivo metabolism of IPN.

GSH conjugation with the enedial metabolite of 4-IPO gave adducts with structures similar to those from the GSH conjugation with **1**, except that the microsomal metabolism of 4-IPO to the enedial was to a lesser extent than the metabolism of IPN to **1**. The adducts characterized include the tricyclic 2′-pyrroline adduct **14**, two mono-GSH pyrrole adducts **16** and **17**, and two bis-GSH pyrrole adducts **18** and **19** (Scheme 3). The bis-GSH pyrrole adducts have been identified by Baer et al. (*9*). Another bis-GSH pyrrole adduct **20** was also detected. In addition to the enedial adducts, an additional metabolite **15** was present in all incubations that contained 4-IPO and NADPH, with or without added nucleophiles. The MS of this product was consistent with an adduct of 4-IPO with NADP. This product is undoubtedly the unknown, non-GSH conjugated, metabolite observed by Buckpitt and Boyd (*6*) in their study of 4-IPO metabolism.

Other products present in the incubation mixture of 4-IPO included **8a**−**b**, **9**, **10b**, **11**, and **12**, derived from sequential oxidation of 4-IPO to IPN then to **1** followed by GSH conjugation. Conversely, GSH adducts derived from the enedial metabolite of 4-IPO were not present in the incubations of IPN. Sequential oxidation of 4-IPO to IPN then to the enedial **1** is likely responsible for some of the toxicity from 4-IPO. The intraperitoneal LD_{50} of 4-IPO in rats increased from 24 mg/kg to 120 mg/kg when the rats were pretreated with pyrazole, an inhibitor of alcohol dehydrogenase, and might be due to the inhibition of the conversion of 4-IPO to IPN (*7*). Interconversion of the four 3-substituted furans (Figure 1) found in mold-damaged sweet potatoes can be achieved chemically (*2*). Similar interconversions of 4-IPO, IPN, and DIOL were observed in the microsomal incubations. Interconversion is likely to occur in vivo where additional enzymes, e.g., alcohol dehydrogenases, are available. However, the three 3-substituted furans studied may not be equally oxidized to enedial metabolites in the microsomal incubations. GSH trapping of the reactive metabolites generated in the incubations indicated that IPN was metabolized to the enedial to the greatest extent, DIOL the least, and 4-IPO fell in between (Figure 2). Only a trace amount of one product was observed in the rat liver microsomal incubation of DIOL, NADPH, and GSH (data not shown).

In conclusion, it is clear that the reactivity of the enedial metabolites of IPN and 4-IPO with thiols and/or amines is responsible for their toxicity. The in vivo metabolism of IPN and 4-IPO is worthy of reinvestigation so as to determine the occurrence of the IPN and 4-IPO interconversion and the predominant scavengers for these reactive enedials in vivo.

Acknowledgment. This research was supported by the Intramural Research Program of the NIH, National Institute of Environmental Health Sciences.

References

(1) Wilson, B. J., Yang, D. T., Boyd, M. R. (1970) Toxicity of mould-damaged sweet potatoes (*Ipomoea batatas*). *Nature. 227*, 521−522.

(2) Boyd, M. R., Burka, L. T., Harris, T. M., and Wilson, B. J. (1974) Lung-toxic furanoterpenoids produced by sweet potatoes (*Ipomoea batatas*) following microbial infection. *Biochim. Biophys. Acta. 337*, 184−195.

(3) Burka, L. T., and Wilson, B. J. (1976) Toxic Furanosesquiterpenoids from Mold-Damaged Sweet Potatoes (*Ipomoea batatas*). In *Mycotoxins and Other Fungal Related Food Problems* (Rodricks, J. V., Ed.) pp. 387-399, American Chemical Society, Washington, D.C.

(4) Rowinsky, E. K., Noe, D. A., Ettinger, D. S., Christian, M. C., Lubejko, B. G., Fishman, E. K., Satorius, S. E., Boyd, M. R., and Donehower, R. C. (1993) Phase I and pharmacological study of the pulmonary cytotoxin 4-ipomeanol on a single dose schedule in lung cancer patients: Hepatotoxicity is dose limiting in humans. *Cancer Res. 53*, 1794−1801.

(5) Boyd, M. R., Burka, L. T., Wilson, B. J., and Sasame, H. A. (1978a) In vitro studies on the metabolic activation of the pulmonary toxin, 4-ipomeanol, by rat lung and liver microsomes. *J. Pharm. Exp. Ther. 207*, 677−686.

(6) Buckpitt, A. R., and Boyd, M. R. (1980) The in vitro formation of glutathione conjugates with the microsomally activated pulmonary bronchiolar alkylating agent and cytotoxin, 4-ipomeanol. *J. Pharm. Exp. Ther. 215*, 97−103.

(7) Boyd, M. R., and Burka, L. T. (1978b) In vivo studies on the relationship between target organ alkylation and the pulmonary toxicity of a chemically reactive metabolite of 4-ipomeanol. *J. Pharm. Exp. Ther. 207*, 687−697.

(8) Alvarez-Diez, T. M., and Zheng, J. (2004) Detection of glutathione conjugates derived from 4-ipomeanol metabolism in bile of rats by liquid chromatography-tandem mass spectrometry. *Drug Metab. Dispos. 32*, 1345−1350.

(9) Baer, B. R., Rettie, A. E., and Henne, K. R. (2005) Bioactivation of 4-ipomeanol by CYP4B1: adduct characterization and evidence for an enedial intermediate. *Chem. Res. Toxicol. 18*, 855−864.

(10) Ravindranath, V., Burka, L. T., and Boyd, M. R. (1984) Reactive metabolites from the bioactivation of toxic methylfurans. *Science. 224*, 884−886.

(11) McClanahan, R. H., Thomassen, D., Slattery, J. T., and Nelson, S. D. (1989) Metabolic Activation of (*R*)-(+)-pulegone to a reactive enonal that covalently binds to mouse liver proteins. *Chem. Res. Toxicol. 2*, 349−355.

(12) Chen, L.-J., Hecht, S. S., and Peterson, L. A. (1995) Identification of cis-2-butene-1,4-dial as a microsomal metabolite of furan. *Chem. Res. Toxicol. 8*, 903−906.
(13) Chen, L.-J., Hecht, S. S., and Peterson, L. A. (1997) Characterization of amino acid and glutathione adducts of cid-2-butene-1,4-dial, a reactive metabolite of furan. *Chem. Res. Toxicol. 10*, 866−874.
(14) Peterson, L. A., Cummings, M. E., Vu, C. C., and Matter, B. A. (2005) Glutathione trapping to measure microsomal oxidation of furan to cis-2-butene-1,4-dial. *Drug Metab. Dispos. 33*, 1453−1458.
(15) Thomassen, D., Pearson, P. G., Slattery, J. T., and Nelson, S. D. (1991) Partial characterization of biliary metabolites of pulegone by tandem mass spectrometry. *Drug Metab. Dispos. 19*, 997−1003.
(16) Chen, L.-J., Lebetkin, E. H., and Burka, L. T. (2003) Metabolism of (*R*)-(+)-menthofuran in F344 rats: Identification of sulfonic acid metabolites. *Drug Metab. Dispos. 31*, 1208−1213.
(17) Rance, M., Sørensen, O. W., Bodenhausen, G., Wagner, G., Ernst, R. R., and Wüthrich, K. (1983) Improved spectral resolution in COSY ^{1}H NMR spectra of proteins via double quantum filtering. *Biochem. Biophys. Res. Commun. 117*, 479−485.
(18) Hwang, T.-L., and Shaka, A. J. (1992) Cross Relaxation without TOCSY: Transverse rotating-frame Overhauser effect spectroscopy. *J. Am. Chem. Soc. 114*, 3157−3159.
(19) John, B. K., Plant, D., and Hurd, R. E. (1993) Improved proton-detected heteronuclear correlation using gradient-enhanced z and zz filters. *J. Magn. Reson., Ser. A 101*, 113−117.
(20) Kay, L. E., Keifer, P., and Saarinen, T. (1992) Pure absorption gradient enhanced heteronuclear single quantum correlation spectroscopy with improved sensitivity. *J. Am. Chem. Soc. 114*, 10663−10665.
(21) Adam, W., Chan, Y.-Y., Cremer, D., Gauss, J., Scheutzov, D., and Scchindler, M. (1987) Spectral and chemical properties of dimethyldioxirane as determined by experiment and ab initio calculations. *J. Org. Chem. 52*, 2800−2803.
(22) Constantino, M. G., and da Silva, G. V. J. (1998) Stereochemistry in substituted cyclopentanes: an approach to the analysis by proton NMR. *Tetrahedron 54*, 11363−11374.
(23) Adam, W., Hadjiarapoglou, L., Mosandl, T., Saha-Möller, C. R., and Wild, D. (1991) Chemical model studies on the mutagenesis of benzofuran dioxetanes in the Ames test: evidence for the benzofuran epoxide as ultimate mutagen. *J. Am. Chem. Soc. 113*, 8005−8011.
(24) Oishi, S., and Nelson, S. D. (1992) Evidence for the formation of heterocyclic arene oxides and γ-keto enal by reaction of menthofuran with dimethyldioxirane. *J. Org. Chem. 52*, 2744−2747.
(25) Ruzo, L. O., Casida, J. E., and Holden, I. (1985) Direct N.M.R. detection of an epoxyfuran intermediate in peracid oxidation of the fungicide methfuroxam. *Chem. Commun.* 1642−1643.
(26) Burka, L. T., and Boyd, M. R. (1985) Furans. In *Bioactivation of Foreign Compounds* (Anders, M. W., Ed.) pp. 243−257, Academic Press, Orlando, FL.
(27) Castagnoli, N., Rimoldi, J. M., Bloomquist, J., and Castagnoli, K. P. (1997) Potential metabolic bioactivation pathways involving cyclic tertiary amines and azaarenes. *Chem. Res. Toxicol. 10*, 924−940.

TX060128F